

# Fully tunable 360° microwave photonic phase shifter based on a single semiconductor optical amplifier

Juan Sancho,\* Juan Lloret, Ivana Gasulla, Salvador Sales, and José Capmany

ITEAM Research Institute, Optical and Quantum Communications Group, Universidad Politécnica de Valencia, Camino de Vera s/n, 46022 Valencia, Spain

\*juasandu@iteam.upv.es

**Abstract:** A fully tunable microwave photonic phase shifter involving a single semiconductor optical amplifier (SOA) is proposed and demonstrated. 360° microwave phase shift has been achieved by tuning the carrier wavelength and the optical input power injected in an SOA while properly profiting from the dispersion feature of a conveniently designed notch filter. It is shown that the optical filter can be advantageously employed to switch between positive and negative microwave phase shifts. Numerical calculations corroborate the experimental results showing an excellent agreement.

©2011 Optical Society of America

**OCIS codes:** (250.5980) Semiconductor optical amplifiers; (070.1170) Analog optical signal processing; (190.4223) Nonlinear wave mixing.

---

## References and links

1. R. W. Boyd and D. J. Gauthier, "Controlling the velocity of light pulses," *Science* **326**(5956), 1074–1077 (2009).
2. R. S. Tucker, P. C. Ku, and C. J. Chang-Hasnain, "Slow-light optical buffers: capabilities and fundamental limitations," *J. Lightwave Technol.* **23**(12), 4046–4066 (2005).
3. J. Capmany and D. Novak, "Microwave photonics combines two worlds," *Nat. Photonics* **1**(6), 319–330 (2007).
4. R. Jakoby, P. Scheele, S. Müller, and C. Weil, "Nonlinear dielectrics for tunable microwave components." 15th International Conference on Microwaves, Radar and Wireless Communications, MIKON-2004 **2**, 369–378, (2004).
5. G. M. Gehring, R. W. Boyd, A. L. Gaeta, D. J. Gauthier, and A. E. Willner, "Fiber based slow-light technologies," *J. Lightwave Technol.* **26**(23), 3752–3762 (2008).
6. T. Baba, "Slow light in photonic crystals," *Nat. Photonics* **2**(8), 465–473 (2008).
7. C. J. Chang-Hasnain and S. L. Chuang, "Slow and fast light in semiconductor quantum well and quantum-dot devices," *J. Lightwave Technol.* **24**(12), 4642–4654 (2006).
8. G. P. Agrawal, "Population pulsations and nondegenerate four-wave mixing in semiconductor lasers and amplifiers," *J. Opt. Soc. Am.* **5**(1), 147–159 (1988).
9. H. Su, P. Kondratko, and S. L. Chuang, "Variable optical delay using population oscillation and four-wave-mixing in semiconductor optical amplifiers," *Opt. Express* **14**(11), 4800–4807 (2006).
10. W. Xue, Y. Chen, F. Öhman, S. Sales, and J. Mørk, "Enhancing light slow-down in semiconductor optical amplifiers by optical filtering," *Opt. Lett.* **33**(10), 1084–1086 (2008).
11. W. Xue, S. Sales, J. Capmany, and J. Mørk, "Wideband 360° microwave photonic phase shifter based on slow light in semiconductor optical amplifiers," *Opt. Express* **18**(6), 6156–6163 (2010).
12. W. Xue, Y. Chen, F. Öhman, and J. Mørk, "The role of input chirp on phase shifters based on slow and fast light effects in semiconductor optical amplifiers," *Opt. Express* **17**(3), 1404–1413 (2009).
13. S. O. Dúill, E. Shumakher, and G. Eisenstein, "The role of optical filtering in microwave phase shifting," *Opt. Lett.* **35**(13), 2278–2280 (2010).</jrm>
14. J. Lloret, F. Ramos, W. Xue, J. Sancho, I. Gasulla, S. Sales, J. Mørk, and J. Capmany, "The influence of optical filtering on the noise performance of microwave photonic phase shifters based on SOAs," *J. Lightwave Technol.* **29**(12), 1746–1752 (2011).

---

## 1. Introduction

The control of the speed of light has attracted considerable attention in the last years due to its intriguing physics and the wide variety of signal processing tasks to which can be applied [1,2]. One of the exciting motivations lays in their potential application to the field of microwave photonics (MWP) [3]. In particular, broadband microwave phase shifters are

needed as a key component in applications such as phased antenna arrays, microwave filters and reconfigurable front-ends [4].

Several photonic technologies have been reported in the literature for the purpose of implementing phase shifting functionalities, including those based on optical fibers [5], photonic crystals [6], and semiconductor waveguides [7]. One of the most successful approaches reported so far is based on the so-called Coherent Population Oscillations (CPO) in Semiconductor Optical Amplifiers (SOA) [8], since it may provide a realistic solution. MWP applications are targeting higher operation frequencies and functionalities that are demanding small devices with low weight and power consumption. Semiconductor based structures provide these features and also allow on-chip integration with other devices while lowering the manufacturing costs.

It has been shown that in CPO based standalone SOA experiments the refractive index dynamics plays no relevant role in the observed microwave phase shift [9]. Hence, the RF phase shift is only governed by the gain dynamics, limiting it to several tens of degrees ( $\sim 30^\circ$  phase advance) and the available RF bandwidth to a few GHz. However, the effects of the refractive index mediated wave mixing can be exploited to increase the degree of the light-speed control by the use of optical filtering prior to detection ( $\sim 150^\circ$  phase shifts at 19 GHz) [10]. Moreover, phase shifts up to  $360^\circ$  at 40 GHz have been recently reached when cascading several SOA based stages [11]. On the other hand, for different modulation chirp values,  $\sim 120^\circ$  phase delay as well as  $\sim 170^\circ$  phase advance at 19 GHz, have been reached by changing the input optical power in a single phase shifter stage [12]. Nevertheless, the combination of both slow and fast light effects is not enough to obtain the desired  $360^\circ$  for many MWP applications.

The previously reported work resorts to the use of optical filters solely to reject the red-shifted sideband aiming at increasing the microwave phase shift. However, the dispersion slope and the amplitude transfer function of the optical filter can play an important role in the total microwave phase shift, as it has been shown in the initial work developed by Ó Dúill et al. [13]. The delay or phase shift incurred by the filter to the RF sideband becomes important since the detected microwave photocurrent depends on the coherent addition of two beat components between the carrier and each RF sideband. Here we show, for the first time to our knowledge, a fully-tunable  $360^\circ$  microwave phase shifter implemented using only one SOA followed by a conveniently designed notch filter. In other words, the scheme proposed in this paper entails saving four SOAs and two optical filters in comparison with the best approach previously reported [11].

## 2. Principle of operation

The amplitude and phase transfer function of the optical filter can be used to enhance the effect of the red-shifted or the blue-shifted sideband resulting in positive or negative microwave phase-shifts, i.e. slow or fast light. In this paper, we have studied the phase and amplitude variations produced by our SOA and consequently we have designed a tailored filter in order to generate the maximum variations of the microwave phase-shifts in combination with the SOA.

Figure 1 shows a general schematic of a photonic phase shifter (PS). The microwave signal modulated on the optical carrier suffers a phase shift as it propagates through the SOA [8]. Optical filtering is included as part of the optical signal processing to enhance the phase shift range [10].

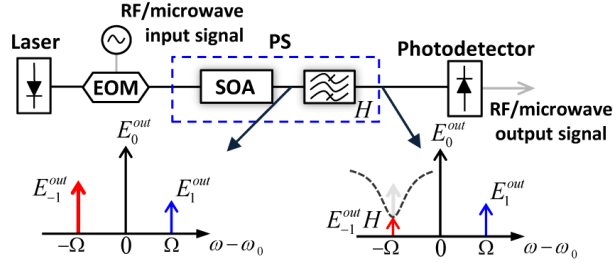


Fig. 1. Schematic of a RF/microwave phase shifter based on SOA and optical filtering.

The microwave phase shift can be tuned by controlling the operation conditions of the SOA as well as the filter dispersion. The use of an optical notch filter, in our case a Fiber Bragg Grating (FBG), allows us to change not only the amplitude but also the phase of the red-frequency shifted-sideband in order maximize the microwave phase shift, Fig. 1. We have considered in our study that the red-shifted sideband is the only spectral component affected by the FBG. Therefore, the bandwidth of the notch filter must be narrower than the modulating frequency.

The electric field at the phase shifter output can be approximated as

$$E^{out}(t, z) = \left( |E_0^{out}| e^{i\phi_0} + |E_1^{out}| e^{-i\Omega t + i\phi_1} + |E_{-1}^{out}| |H| e^{i\Omega t + i\phi_{-1} + i\phi_H} \right) e^{-i(\omega_0 t - k_0 z)}, \quad (1)$$

where  $\omega_0$  is the frequency of the optical carrier,  $k_0$  is the propagation constant of the carrier, and  $\Omega$  is the modulation frequency.  $E_0^{out}$ ,  $E_1^{out}$  and  $E_{-1}^{out}$  are respectively the complex amplitudes of the carrier, blue and red-shifted sideband, while  $\phi_0$ ,  $\phi_1$  and  $\phi_{-1}$  are the corresponding optical phase features. Based on the weak modulation assumption, the higher order sidebands are neglected. The modulus and phase components of the filter transfer function are represented by  $|H|$  and  $\phi_H$  respectively. Due to the beating between the optical waves in the photodetector, the photocurrent at modulation frequency  $\Omega$  is proportional to

$$i(\Omega) \propto |E_0^{out}| |E_1^{out}| e^{i(-\phi_0 + \phi_1)} + |E_0^{out}| |E_{-1}^{out}| |H| e^{i(\phi_0 - \phi_{-1} - \phi_H)}. \quad (2)$$

The phase shift of the microwave signal is determined by  $\arg\{i(\Omega)\}$  minus a phase reference, normally corresponding to the phase obtained at the minimum input power or injection current [10].

Figure 2(a) and 2(b) illustrate the evolution of the signal complex phasors in a polar representation, by controlling the injection current of the SOA. The blue phasor represents the evolution of the first photocurrent term of Eq. (2) (the beat between the carrier and the blue-shifted sideband), the red phasor corresponds to the second term (the beat between the carrier and the filtered red-shifted sideband) and finally the black phasor represents the total microwave photodetected signal. The dotted phasors indicate the reference point. Figure 2(a) illustrates the results reported in previous work [10]. The optical filter attenuates the red-shifted sideband and a large variation of positive phase shifts is created. However, as shown in Fig. 2(b), by inducing the proper amplitude and phase change on the red-shifted sideband, it is possible to achieve negative phase shifts. Thus, the desired  $360^\circ$  phase shift range can be achieved by combining the SOA output with a tailored filter providing the desired phase and amplitude changes on the red-shifted sideband.

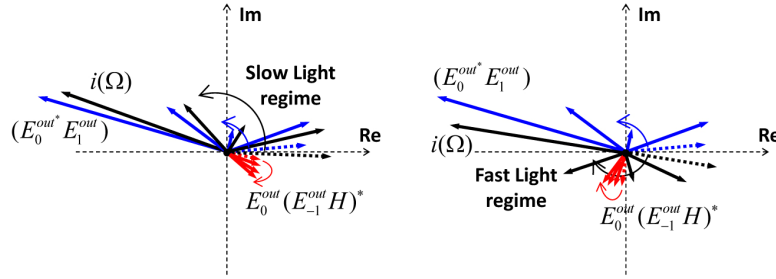


Fig. 2. Illustrations of the evolution of the complex phasors in a polar representation for two cases: (a) when the red-shifted sideband is only attenuated and (b) when it is attenuated and also phase shifted.

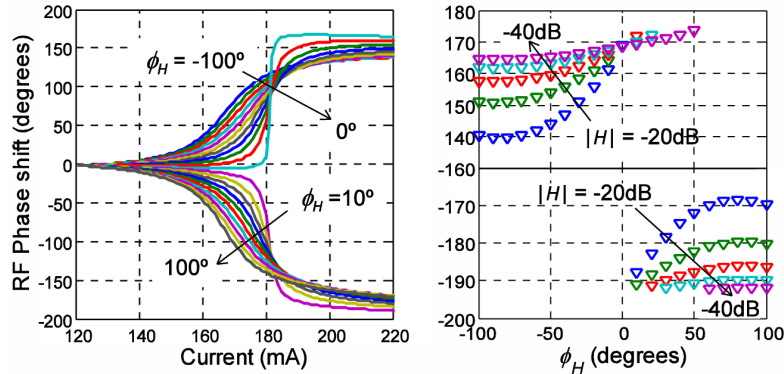


Fig. 3. (a) Calculated RF phase shifts as a function of the injection current as well as the  $\phi_H$ . (b) Maximum values of phase shift as a function of  $\phi_H$  and  $|H|$ .

Numerical calculations of the RF/microwave phase shift as a function of the attenuation and phase induced by the photonic notch filter are shown in Fig. 3. The following main parameters of the SOA are used [9]:  $P_{sat} = 4\text{dBm}$ ,  $\tau_s = 140\text{ps}$ ,  $\alpha = 6$ ,  $\Gamma = 0.45$ ,  $\gamma = 3000\text{m}^{-1}$ ,  $P_{in} = 0\text{dBm}$ ,  $\Omega = 20\text{GHz}$ ,  $L = 1000\mu\text{m}$ . All phase shifts are obtained upon increasing the injection current from 100 mA to 200mA. Figure 3(a) shows the different RF phase shifts when the attenuation of the filter is fixed to  $-20\text{dB}$  and the phase induced on the red-shifted sideband ( $\phi_H$ ) is tuned from  $-100^\circ$  to  $100^\circ$ . It is easy to infer the existence of a high dependence on the phase parameter. When  $-100^\circ \leq \phi_H \leq 0^\circ$  slow light effect is observed inducing positive phase shifts. However, when  $10^\circ \leq \phi_H \leq 100^\circ$ , fast light behavior is achieved which induces a negative RF phase shift. On the other hand, Fig. 3(b) depicts the total RF phase shift versus the filter-induced phase shift for different attenuation values. As observed, an increase of the red-shifted sideband attenuation is accompanied by an increase in the RF phase shift. Thus, there are less filter phase constraints to obtain the full  $360^\circ$ .

The novel proposed phase shifter configuration is quite flexible in terms of the number of parameters that can be changed to achieve the desired  $360^\circ$  phase excursion. For instance, Fig. 4 shows the evolution of the RF phase shift for different optical power levels at the SOA input. The attenuation of the red-shifted sideband has been kept to a constant value of  $30\text{dB}$  as well as the induced phase ( $\phi_H$ ) to  $20^\circ$ . By tuning just the SOA input power and the SOA injection current, phase shift changes from negative to positive can, again, be obtained.

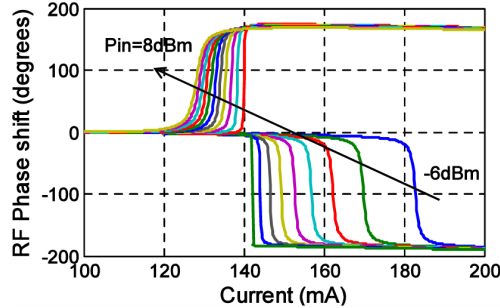


Fig. 4. Calculated RF phase shifts induced by increasing the optical power at the SOA input as a function of the injection current.

### 3. Experimental results

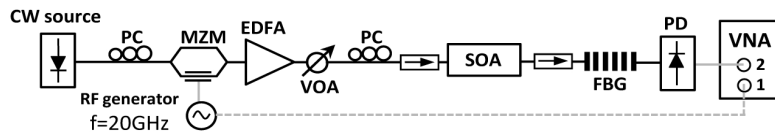


Fig. 5. Experimental set-up.

We have experimentally investigated the proposed  $360^\circ$  phase shifter configuration using the set-up depicted in Fig. 5. A CW laser emitting at 1556 nanometers was modulated using a microwave tone at 20 GHz by means of an external zero-chirp Mach-Zehnder modulator. The non-linear SOA device was designed to have a low saturation output power of 4 dBm. The phase shift impressed on the microwave signal will be electrically controlled by means of the injection current. To adjust the SOA input power in our measurements, we have used an EDFA booster and a variable optical attenuator (VOA). At the SOA output, a FBG operating in transmission was used to implement the notch filter. The FBG can provide attenuation greater than 40 dB with a  $-3$  dB bandwidth of approximately 10 GHz (see Fig. 6). The optical signal is photodetected and acquired by means of a vectorial network analyzer. The polarization controller (PC) placed before the SOA has been used to maximize the CPO effect.

The contour plots in Fig. 6(a) represent the experimental results for the microwave phase shift as a function of the SOA injection current, as well as the spectral position of the red-shifted sideband within the FBG. The red markers of Fig. 6(b) show the variation of the amplitude and phase induced in the red-shifted sideband due to the FBG. They correspond to an attenuation of  $\sim 40$  dB and a phase shift from  $20^\circ$  to  $80^\circ$ . The results have been measured for two optical powers at the SOA input: 0 and 2 dBm. The targeted frequency areas are labeled as phase advance and delay. More than  $360^\circ$  can be accomplished just by tuning 2 dB the optical input power and only 1 GHz the laser wavelength.

Figure 7 illustrates the experimental validation (markers) and the theoretical (solid lines) results for the phase shift and power variation induced by slow and fast light effects through sweeping the injection current of the SOA for two different optical input powers. Figure 7 shows a perfect agreement between the theoretical results and the experimental data for both RF/microwave phase shift and power. The initial reference phase is chosen for a SOA injection current of 200 mA and 0 dBm of SOA optical input power. The laser wavelength has been chosen to induce an additional phase shift of  $60^\circ$  and an attenuation of 40 dB to the red-shifted sideband produced by the FBG. Just by tuning the SOA injection current,  $180^\circ$  RF/microwave phase shift can be tuned. The additional  $180^\circ$  are induced by increasing 2 dB the optical input power. As expected, the sharp increase of the phase shift corresponds to a deep dip in the RF power. Mechanisms to equalize this power loss are under current investigation.

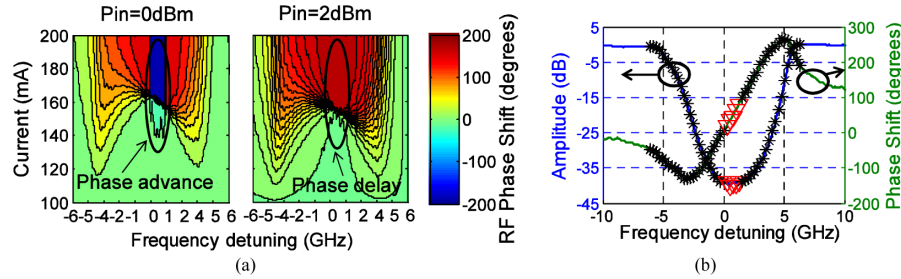


Fig. 6. (a) Measured RF phase shift as a function of both SOA input current and FBG frequency detuning for two different optical powers at the SOA input. (b) Measured FBG amplitude and phase response.

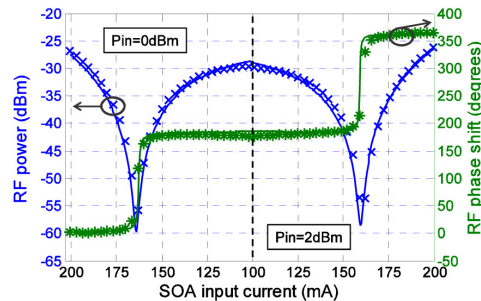


Fig. 7. Theoretical (lines) and experimental (markers) photodetected RF power and phase shift as function of the SOA input current when the input power is fixed at 0dBm and 2dBm.

## 5. Conclusions

In conclusion, we have experimentally investigated the slow and fast light effects induced by the optical filtering stage placed at the SOA output in tunable microwave phase shifter. To the best of our knowledge, this is the first realization of a fully tunable  $360^\circ$  microwave phase shifter based on slow and fast light effects using a single SOA. The proposed scheme saves four SOAs and two optical filters compared to the best scheme previously reported [11]. It doesn't reduce only de complexity but also the deterioration in terms of noise levels [14]. Since the blue-shifted sideband at the SOA output has a power dip on the phase transition, the attenuated red-shifted sideband, with the proper phase, can change the behavior of the phase shifter. In order to obtain an increase of the total phase shift by adding both effects, slow and fast light, an abrupt phase transition and, therefore a high deep notch is required. Numerical calculations and experimental results show excellent agreement. Up to  $360^\circ$  phase shift has been experimentally demonstrated using two different optical powers at the SOA input by properly adjusting the frequency detuning of the optical filter. This is highly desired for many microwave photonic applications, such as microwave photonic filters and antenna beamsteering. The phase shifter bandwidth, as well as the operating frequency, is strongly dependent on the filtering scheme. It has to ensure that at a certain frequency range the fast light condition is met. In our particular case, within a bandwidth greater than 1GHz can be achieved. Narrower filters would allow operating at lower frequencies but at the cost of using less frequency bandwidth. Investigations are being conducted to achieve broadband operation and provide output power equalization.

## Acknowledgments

The authors wish to acknowledge the financial support of the European Commission Seventh Framework Programme (FP7) project GOSPEL; the Generalitat Valenciana through the Microwave Photonics research Excellency award programme GVA PROMETEO 2008/092 and also the Plan Nacional I + D TEC2008-06145.